Available online at www.sciencedirect.com
ScienceDirect
Journal of Power Sources 158 (2006) 1365–1372
JOURNAL OF POWER SOURCES
www.elsevier.com/locate/jpowsour

Comparative performances for primary lithium batteries of some covalent and semi-covalent graphite fluorides

Jérôme Giraudet [a], Céline Delabarre [a], Katia Guérin [a], Marc Dubois [a], Francis Masin [b], André Hamwi [a,*]

[a] *Laboratoire des Matériaux Inorganiques, UMR CNRS 6002, Université Blaise Pascal, 24 av. des Landais, 63177 Aubière Cedex, France*
[b] *Matière Condensée et Résonance Magnétique, Université Libre de Bruxelles, CP 232, Boulevard du Triomphe, B-1050 Bruxelles, Belgium*

Received 20 July 2005; received in revised form 29 September 2005; accepted 10 October 2005
Available online 15 November 2005

Abstract

Different graphite fluorides were prepared by three different synthesis ways: fluorination at room temperature, at 600 °C, and refluorination at 400 and 530 °C of a fluorinated graphite prepared at room temperature. All the samples have been characterized by ^{19}F MAS NMR and FT-IR spectroscopies. Their electrochemical performances as cathode materials in primary lithium batteries have been investigated at room temperature and at 60 °C and as a function of the current density. Ageing behavior has been also studied using some liquid electrolytes. Refluorinated sample at 400 °C exhibits the best performances because of both its good average discharge potential and its discharge capacity, i.e. 2.54 V and 848 Ah kg^{-1}, respectively. For this sample, the best specific energy density and specific power density are 2149 Wh kg^{-1} and 902 W kg^{-1}, respectively.

Keywords: Fluorination; Graphite fluoride; Fluorine–graphite intercalation compounds; Primary lithium batteries; Electrochemical properties

1. Introduction

The development of portable electronic systems has led to many researches on electrode materials for lithium cells with the goal to significantly improve discharge capacity, discharge potential and cyclability. Fluorine–graphite intercalation compounds and graphite fluorides (CF_x) are interesting candidates for primary lithium batteries [1–4]. Indeed, the open circuit voltage (OCV) of the theoretical Li/F_2 cell is close to 6 V. In practice, electrochemical systems associating lithium and fluorinated carbon materials exhibit high OCV, higher than 3.2 V, depending of the C–F bond character (covalent, semi-covalent or ionic). The OCV is inversely proportional to the C–F bond covalence, the highest OCV is obtained for ionic bonding [2–6]. The three bonding are obtained from three ways of synthesis.

Ionic bonding: fluorine–graphite intercalation compounds (fluorine–GIC, C_xF with low fluorine content: $x > 4$) obtained at temperatures below 100 °C using a mixture of fluorine with either HF [7] or volatile fluorides MF_n (BF_3, IF_5, IF_7, WF_6, ...) [8].

Semi-covalent bonding: fluorine–GIC, C_xF with $2 < x < 4$, obtained by an increase of the fluorine content with the previous synthesis [9] or for fluorinated graphites prepared at room temperature using a mixture of fluorine with HF and volatile fluorides MF_n [10,11] and whose general chemical formula is $CF_x(MF_n)_y$ ($0.5 \leq x \leq 0.9$; $0.06 \geq y \geq 0.02$).

Covalent bonding: graphite fluorides achieved from direct fluorination of graphite in the 350–600 °C temperature range [12,13]. Their chemical composition is $(C_xF)_n$ with $x = 1$ or 2 for temperature synthesis of 600 and 350 °C, respectively. Recently, in our laboratory, it has been underlined that a thermal refluorination, performed at temperatures higher than 400 °C, of semi-covalent CF_x results in new covalent graphite fluorides exhibiting structural characteristics close to those of $(CF)_n$ obtained for direct fluorination at 600 °C [14,15]. However, the content of structural defects is lowered, dangling bonds amounts being significantly lowered by refluorination.

* Corresponding author. Tel.: +33 473 407 103; fax: +33 473 407 108.
E-mail addresses: andre.hamwi@univ-bpclermont.fr (A. Hamwi), jerome.giraudet@univ-bpclermont.fr (J. Giraudet), celine.delabarre@univ-bpclermont.fr (C. Delabarre), katia.guerin@univ-bpclermont.fr (K. Guérin), marc.dubois@univ-bpclermont.fr (M. Dubois), fmasin@ulb.ac.be (F. Masin).

0378-7753/$ – see front matter © 2005 Elsevier B.V. All rights reserved.
doi:10.1016/j.jpowsour.2005.10.020

Conventional covalent graphite fluorides $(CF)_n$ used in commercial lithium batteries possess a discharge capacity of about 900 Ah kg^{-1} and a discharge potential close to 2.1 V [1–3]. As for OCV, average discharge potential is higher for less covalent materials, e.g. for $CF_x(MF_n)_y$. In particular when $MF_n = IF_5$ is used as catalyst fluoride, the discharge potential increases up to 3 V [4,16–18]. Nevertheless, this increase is associated with a capacity decrease due to a poorly fluorine content ($0.5 < x < 0.9$). After thermal treatment under F_2 these graphite fluorides exhibit interesting electrochemical characteristics; indeed, high capacities are reached, about 900 Ah kg^{-1}, and the discharge potentials are significantly increased in comparison to commercial ones (2.54/2.10 V versus Li^+/Li). However, discharge potentials are lower than for semi-covalent CF_x, the modulation is performed through the refluorination temperature. Higher the refluorination temperature higher the C–F bond covalence, this results in a potential decrease [19].

Furthermore, an important key point for an industrial application is to prevent electrochemical characteristics from fading during long time storage. Such storage effect is evidenced by the study of the evolution of the electrochemical behavior upon ageing. Specific applications may also require high specific energy or strong specific power.

In this work, we investigated in details the electrochemical behavior of covalent graphite fluorides obtained by refluorination of semi-covalent CF_x. In particular, the performances of these materials when high current densities are applied and upon ageing are reported. In addition, similar electrochemical tests, performed on commercial covalent $(CF)_n$ and semi-covalent CF_x, are also presented for comparison. Preliminary, C–F bonding characterization of all the studied samples is necessary to better understand the electrochemical mechanisms.

2. Experimental

2.1. Sample preparation

The starting material was a natural graphite powder from Madagascar with average grain size of about 4 μm, the best results in terms of fluorination efficiency were obtained for this graphite. First, fluorine–graphite intercalation compound, denoted $CF_x(IF_5)$, was prepared according to a room temperature synthesis using iodine fluoride (IF_5), hydrogen fluoride (HF) and fluorine (F_2) gaseous mixture as described in Ref. [10]. Refluorination of $CF_x(IF_5)$ was carried out under pure F_2 gas at 400 and 530 °C, resulting in samples denoted CF(400) and CF(530), respectively [14,15]. The conventional covalent graphite fluoride, denoted CF(HT), was synthesized at 600 °C under pure F_2 gas flow [13]. According to weight uptake, the following chemical formula were obtained: $CF_{1.02}$, $CF_{0.83}$, $CF_{0.98}$ and $CF_{1.10}$ for, respectively, $CF_x(IF_5)$, CF(400), CF(530) and CF(HT). As previously shown [14,15], for raw material or for the lower refluorination temperature, a part of mass uptake was in fact assigned to residual catalyst iodine fluorides and not to fluorine atoms: for example, for $CF_x(IF_5)$, the true chemical formula obtained by chemical analysis was $CF_{0.73}(IF_5)_{0.02}(HF)_{0.06}$ [14].

2.2. Characterization

^{19}F magic angle spinning (MAS) nuclear magnetic resonance (NMR) experiments were performed on a Bruker MSL 300 spectrometer (working frequency of 282.2 MHz) with a 4 mm cross polarization/magic angle spinning probe from Bruker working at 12 kHz. A simple sequence (τ-acquisition) was used with a $\pi/2$ pulse length of 4 μs. The external reference was CF_3COOH, all chemical shifts were referenced with respect to $CFC1_3$ ($\delta_{CF_3COOH} = -78.5$ ppm versus δ_{CFCl_3}).

Fourier transform infrared spectroscopy (FT-IR) was performed using a SHIMADZU FT-IR-8300 spectrometer; the spectra were recorded in a dry air atmosphere between 400 and 4000 cm^{-1} with 20 spectra accumulation through a pellet (2 mg of the sample material diluted in 200 mg of KBr).

2.3. Electrochemical study

Typical electrodes were composed of graphite fluoride (about 80% by weight, w/w), graphite powder (10%, w/w) to insure electronic conductivity and polyvinylidene difluoride (PVDF, 10%, w/w) as binder. After stirring in propylene carbonate (PC), the mixture was spread uniformly onto a stainless steel current collector disk of 10 mm in diameter. Finally, after the PC evaporation the disk was heated, under vacuum at 150 °C for 2 h, to remove traces of water and solvent. The mass of active material was close to 2 mg for all the experiments. A two electrodes cell was used (Swagelok cell type), where lithium was both reference and counter electrode. A PVDF microporous film wet with electrolyte composed of a 1 mol L^{-1} of a lithium salt ($LiClO_4$ or $LiBF_4$) dissolved in PC (doubly distilled) or in mixed electrolyte PC–ethylene carbonate (EC) (1:1 volumic ratio), was sandwiched between the composite electrode and a lithium metal foil. The cells were assembled in an argon filled dried glove box. Relaxation was performed for at least 2 h until OCV stabilization. Galvanostatic discharges, carried out on a VMP2–Z from Biologic, under current densities ranged between 10 and 960 A kg^{-1}, were acquired at room temperature or at 60 °C between the initial OCV and 1.5 V. Discharge capacities detailed in this article have been obtained for a cell cut-off of 1.5 V. Ageing of materials are simulated by putting the cells at 60 °C for 5 days before electrochemical measurements.

3. Results and discussion

3.1. C–F bonding

Prior to electrochemical tests, the F/C molar ratio and the C–F bonding must be investigated because these two main parameters characterize the synthesis efficiency and then the electrochemical properties. So, FT-IR and ^{19}F MAS NMR spectroscopies have been used as they are excellent probes for the bonding determination.

Between 400 and 2000 cm^{-1}, the FT-IR spectra (Fig. 1a) show vibration bands at 1135 and 1215 cm^{-1}. For $CF_x(IF_5)$, the weak band at 1135 cm^{-1} is attributed to semi-covalent C–F bond vibration [10], its small intensity is related to the conductor

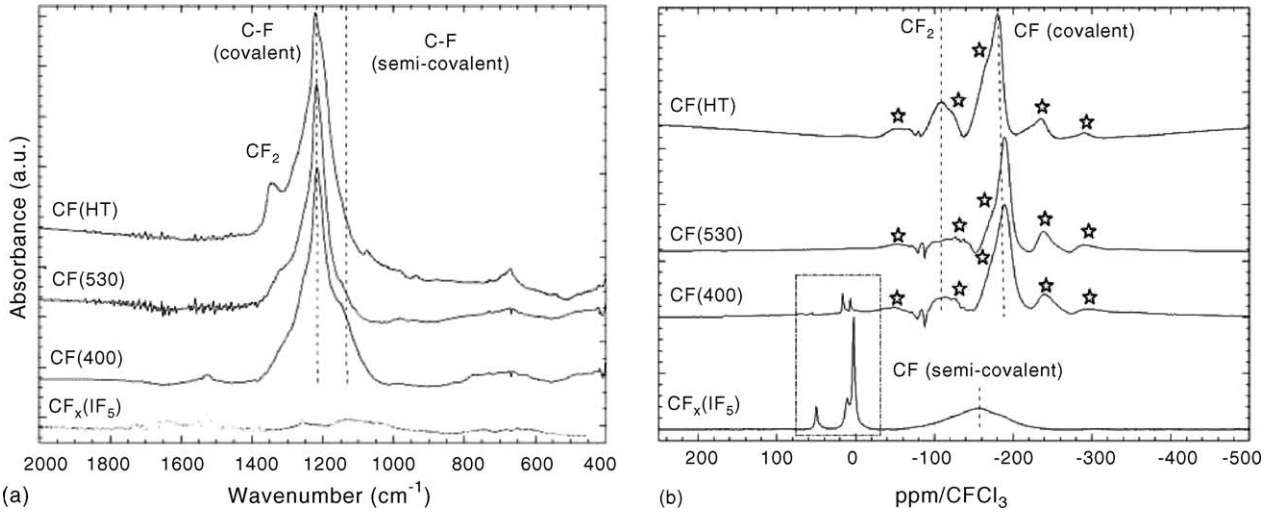

Fig. 1. (a) FT-IR spectra of $CF_x(IF_5)$, CF(400), CF(530) and CF(HT). (b) ^{19}F MAS spectra, at 12 kHz, of $CF_x(IF_5)$, CF(400), CF(530) and CF(HT). Stars denote spinning sidebands.

character of the sample. On CF(400) and CF(530) spectra, two bands are observed, the intense one at 1215 cm^{-1} is assigned to covalent C–F bond [13]. Semi-covalent contribution appears only as a shoulder of the covalent one. The effect of the increase of the refluorination temperature consists in the disappearance of the semi-covalent character which occurs simultaneously with the improvement of the covalence as evidenced for CF(530). For CF(HT), in addition to the signal of covalent C–F at 1215 cm^{-1}, an additional peak at 1380 cm^{-1} is related to CF_2 groups [13]. In the case of CF(400) and CF(530), the content of CF_2 group is increased with refluorination temperature but it is still low in comparison with CF(HT). This CF_2 groups are assigned either to fluorine atoms located at the edge of graphite layers or to structural defects.

The room temperature ^{19}F MAS NMR spectra (Fig. 1b) exhibit several lines. First, for CF(HT), CF(400) and CF(530) spectra in the −40/−340 ppm range, two isotropic lines at −119 and −189 ppm are present with their spinning sidebands. In agreement with FT-IR results, the line at −189 ppm corresponds to fluorine atoms involved in covalent C–F bonds. The second one at −119 ppm confirms the presence of CF_2 groups [20]. The CF_2 content is smaller for CF(400) and CF(530) than for CF(HT) whereas for $CF_x(IF_5)$ these groups are absent. This CF_2 content variation by comparison with CF(HT) is explained either by the graphite layers size (small size results in higher CF_2/CF ratio) or by the presence of structural defects. As expected, the typical chemical shift of semi-covalent C–F bond in $CF_x(IF_5)$ is observed at −160 ppm [21,22]. In the 80/−40 ppm range, $CF_x(IF_5)$ and CF(400) spectra show narrow lines which are assigned to residual catalyst: IF_5 groups resonance line appears as a doublet at 2 and 50 ppm whereas IF_6^- chemical shift was measured at 10 ppm [23–26]. Moreover, as already described, iodine fluorides content decreases with refluorination temperature; at 400 °C the content is low while at 530 °C, iodine fluorides have been entirely removed from the fluorocarbon matrix [14,15,22].

By combination of FT-IR and ^{19}F NMR spectroscopies, a characterization of both the C–F bonding and the kind of fluorocarbon groups has been performed. Room temperature CF_x possesses semi-covalent C–F bonds as evidenced by the IR band at 1135 cm^{-1} and the NMR line at −160 ppm. For the other samples, CF(400), CF(530) and CF(HT), i.e. with a high temperature of synthesis or of refluorination, the C–F bonding evolves towards a covalent character. This change is underlined by the shift of the C–F resonance line from −160 to −190 ppm [14,15,22]. IR data confirms this evolution because of the shift of the band at 1215 cm^{-1} for covalent character. In addition, these spectroscopies underline the presence of CF_2 groups.

In the following sections, the electrochemical properties will be investigated and rely to the C–F bonding, the effect of the presence of CF_2 groups on these properties will also be discussed.

3.2. Electrochemical properties

3.2.1. Galvanostatic discharges at low current density

Fig. 2a represents the galvanostatic discharge curves, of the studied samples, obtained at room temperature for 10 A kg^{-1} current density using 1 M $LiClO_4$/PC electrolyte. The flat curve evolution is typical for this material family [1–4]. The average discharge potential $E_{1/2}$, which is the potential measured at half discharge capacity, is equal to 3.13, 2.54, 2.34 and 2.02 for $CF_x(IF_5)$, CF(400), CF(530) and CF(HT), respectively. This discrepancy is induced by different electrode polarizations during the electrochemical reduction. This polarization is related to reaction (1) consisting in the C–F bond dissociation through LiF formation.

$$CF_x + xLi^+ + xe^- \rightarrow C + xLiF \quad (1)$$

As shown by ^{19}F NMR and FT-IR, the covalent character σ evolves as follow: $\sigma_{CF_x(IF_5)} < \sigma_{CF(400)} < \sigma_{CF(530)} < \sigma_{CF(HT)}$,

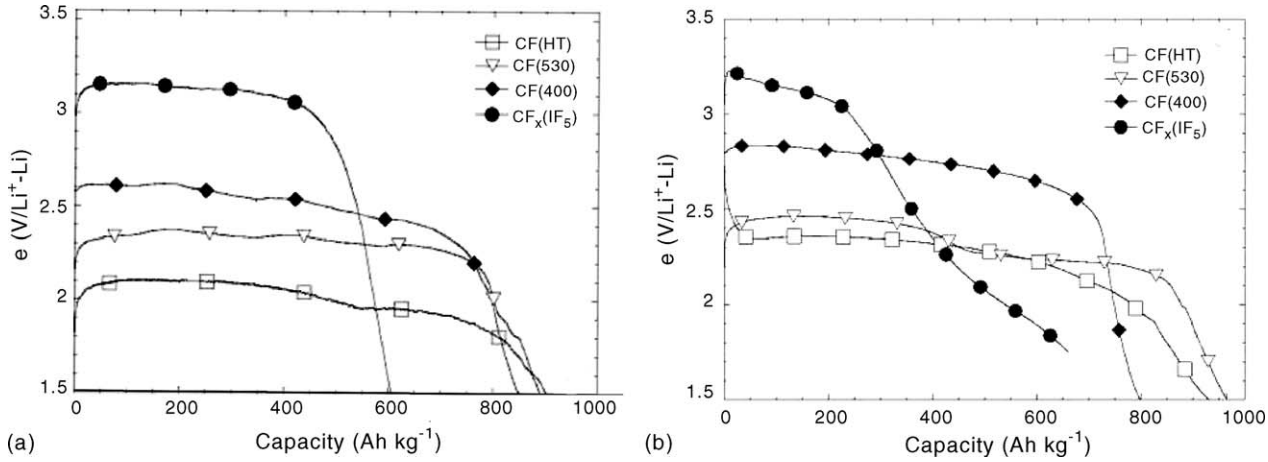

Fig. 2. Galvanostatic discharge curves (10 A kg^{-1}, 1 M $LiClO_4$/PC) of $CF_x(IF_5)$, CF(400), CF(530) and CF(HT) at room temperature (a) and at 60 °C (b).

and explains the average discharge potential obtained. The higher the bonding energy, i.e. the covalence, the higher the polarization, and consequently the lower the discharge potential.

The discharge capacities are closed for covalent samples, about 850–900 Ah kg^{-1}. Theoretical capacities, based on chemical composition and calculated from Eq. (1), are given in Table 1 (all experimental capacities are given with an error of ±5%). Experimental and theoretical capacities are of the same magnitude, the difference (positive or negative) may be explained by different processes. First, in Section 3.1, we demonstrated the presence of CF_2 groups, which are taken into account for fluorine content; they are known to be electrochemically inactive (because they require too much energy to be reduced). These CF_2 groups then lead to experimental capacities diminution in comparison to the theoretical ones. On the other hand, an opposite behavior can be observed taking into account the creation, during lithium intercalation, of an intermediary phase which could accommodate more than one lithium by fluorine atom (Eq. (2)).

$$CF_x + (x+\varepsilon)Li^+ + (x+\varepsilon)e^- \rightarrow Li_{x+\varepsilon}CF_x \quad (2)$$

"$Li_{x+\varepsilon}CF_x$" species is unstable and rapidly turns into LiF and a secondary compound involving lithium ions and defluorinated carbonaceous material $Li_\varepsilon C$ according to the reaction (3):

$$Li_{x+\varepsilon}CF_x \rightarrow xLiF + Li_\varepsilon C \quad (3)$$

Table 1
Theoretical and experimental (at RT and at 60 °C) discharge capacities of compounds used in lithium batteries

Sample	$CF_x(IF_5)$	CF(400)	CF(530)	CF(HT)
x in CF_x	0.73	0.83	0.98	1.10
Theoretical capacity (Ah kg^{-1})	756	801	858	896
RT experimental capacity (Ah kg^{-1})[a]	609	848	891	905
60 °C experimental capacity (Ah kg^{-1})	661 (at 1.75 V)	800	965	929

[a] Li//1 M $LiClO_4$/PC//CF_x, 10 A kg^{-1}.

For $CF_x(IF_5)$, the presence of residual iodine fluorides could hinder lithium diffusion leading to an experimental capacity decrease: 609 Ah kg^{-1} at room temperature to be compared with the theoretical one of 756 Ah kg^{-1}.

In order to favour the lithium diffusion, electrochemical tests are also performed at 60 °C. Galvanostatic discharges acquired at 60 °C (Fig. 2b) show an increase of the discharge potentials without significant capacities change. A higher temperature improves the kinetic of lithium intercalation by increase of the lithium diffusion. The electrode polarization is then smaller. A different evolution appears for $CF_x(IF_5)$ discharge curve, constituted of two successive regions with different slopes, the first one being flatter than the second. Presence of iodine fluorides is prejudicial for lithium batteries, indeed these fluorides react with battery components such as current collectors and electrolyte; at room temperature this results in self discharge [19]. At 60 °C, reactivity is increased resulting in a progressive deterioration of lithium cell which explains the continuous voltage decrease of the second part of the curve.

3.2.2. Galvanostatic discharges upon ageing

An important point for marketing of electrode materials is a good ageing of the lithium cells based on this materials: electrochemical properties must not be affected by long time storage between manufacturing and discharge into an electronic system. Ageing is simulated by putting lithium cell at 60 °C for 5 days. During this period, reactivity and thermal stability of both salt and solvent in the presence of the active material influence the future electrochemical properties. Four different electrolytes composed of two salts ($LiClO_4$ and $LiBF_4$) and two solvents (EC and mixed EC–PC) are tested. This choice is related to the fact that they are commonly used in lithium batteries. Ageing of $CF_x(IF_5)$ always leads to cell deterioration due to chemical reaction of iodine fluorides with battery components, so, electrochemical properties are not available. Fig. 3 reports the room temperature galvanostatic discharge under 10 A kg^{-1} after 5 days at 60 °C for all electrolytes. Whatever the sample both the highest discharge potentials and capacities are obtained for 1 M $LiClO_4$/PC–EC. Furthermore, the values obtained for 1 M $LiClO_4$/PC are close for tests with and without ageing. When

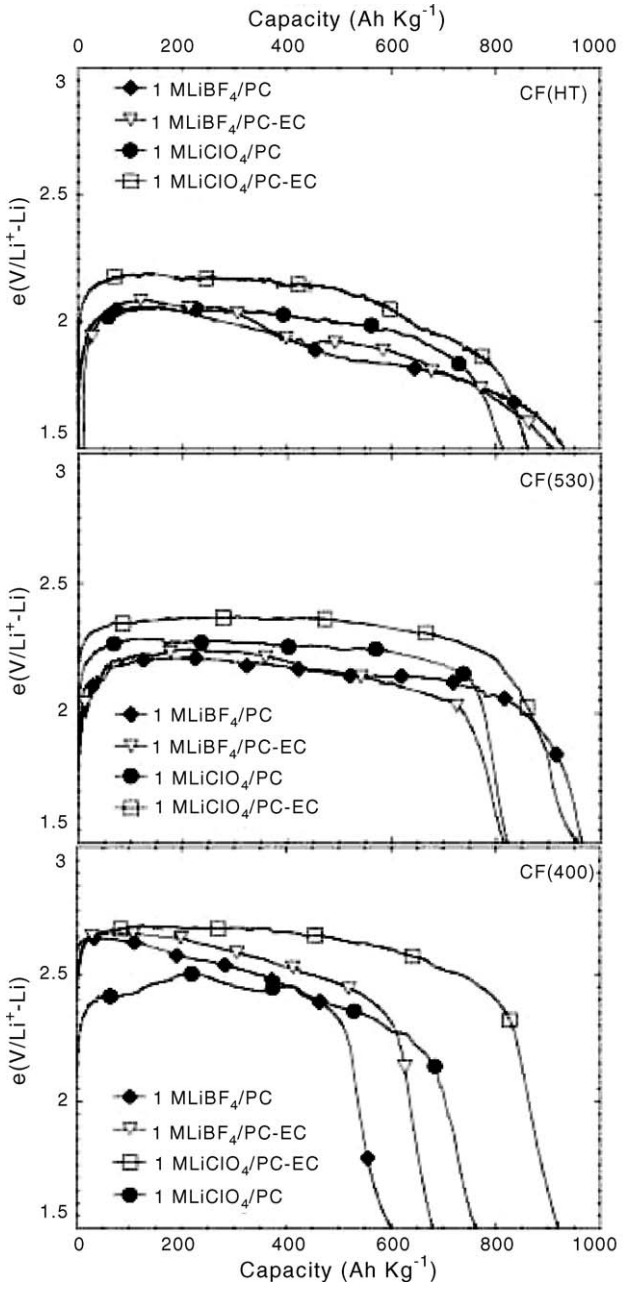

Fig. 3. Galvanostatic discharge curves (10 A kg^{-1}, RT) after ageing (5 days, 60 °C) for different electrolytes (1 M $LiClO_4$/PC, 1 M $LiClO_4$/PC–EC, 1 M $LiBF_4$/PC and 1 M $LiBF_4$/PC–EC).

$LiBF_4$ based electrolytes are used for ageing experiments the lower potentials are measured. The potential gap for discharge with these different electrolytes is larger than for similar studies without ageing, 0.25 V instead of less than 0.1 V without ageing [19].

In the previous study, this gap was explained by the difference in the ionic conductivity of the electrolyte; here, we must also take into account the thermal stability of the salt. Solvent degradation products on the electrode surface and/or cointercalated solvent molecules, may hinder lithium diffusion. Such phenomena are at the origin of the lesser lithium intercalation level. Indeed for CF(530) and CF(HT), no important capacity variation appears, about 10% and inferior to 10%, respectively. In opposite, for CF(400) capacity variation is close to 30%; the presence of residual fluoride catalyst leads to an enhancement of the solvent degradation. As the iodine species content is very low for CF(400) [15], such a process can not be only related to the iodine removal from the material towards the electrolyte. The degradation processes seem to occur within the interlayer space where IF_n species are located. For CF(400), a complete physicochemical characterization (^{19}F, ^{13}C high resolution NMR, FT-IR and EPR) underlines a hybrid structure in which semi-covalent and covalent C–F bonds coexist, i.e. sp^2 and sp^3 carbon atoms thanks to the presence of residual iodine species [14,15,22]. The reaction of IF_n with the electrolyte could occur in the regions where the planarity of the graphene is conserved resulting in a partial exfoliation of the electrode material. So, a part of the electrode material could be lost for electric connection. Another hypothesis consists in the accumulation of electrolyte decomposition products trapped between the fluorocarbon layers leading to lithium diffusion hindrance as previously proposed. Both the two hypothesis remain to be verified. However, solvent degradation can be avoided by the use of co-solvent such as PC–EC mixture. Contrary to PC which may favour solvated lithium cointercalation by strong solvent-ion interaction, PC–EC seems to lower such phenomenon. So, the use of 1 M $LiClO_4$/PC–EC constitutes a technological solution to reduce electrochemical properties fading during long storage.

In Table 2, is reported the effect of the elimination of the degradation products by placing the aged cathode material in a new cell with new electrolyte and new polymer separator. The working electrode is extracted from ageing cell and dried in glove box. Capacity and potential discharge values obtained are both included between ageing and not ageing data. After reassembling, potential do not entirely recover the non-aged values, all degradation products cannot be entirely removed by this

Table 2
Discharge potential and capacity for different experimental conditions

Sample	No ageing		After ageing		After ageing and reassembling	
	$E_{1/2}$ (V)	Capacity (Ah kg^{-1})	$E_{1/2}$ (V)	Capacity (Ah kg^{-1})	$E_{1/2}$(V)	Capacity (Ah kg^{-1})
CF(530)	2.34	891	2.26	821	2.30	836
CF(400)	2.54	848	2.43	764	2.47	830

Li//1 M $LiClO_4$/PC//CF_x, 10 A kg^{-1}, RT.

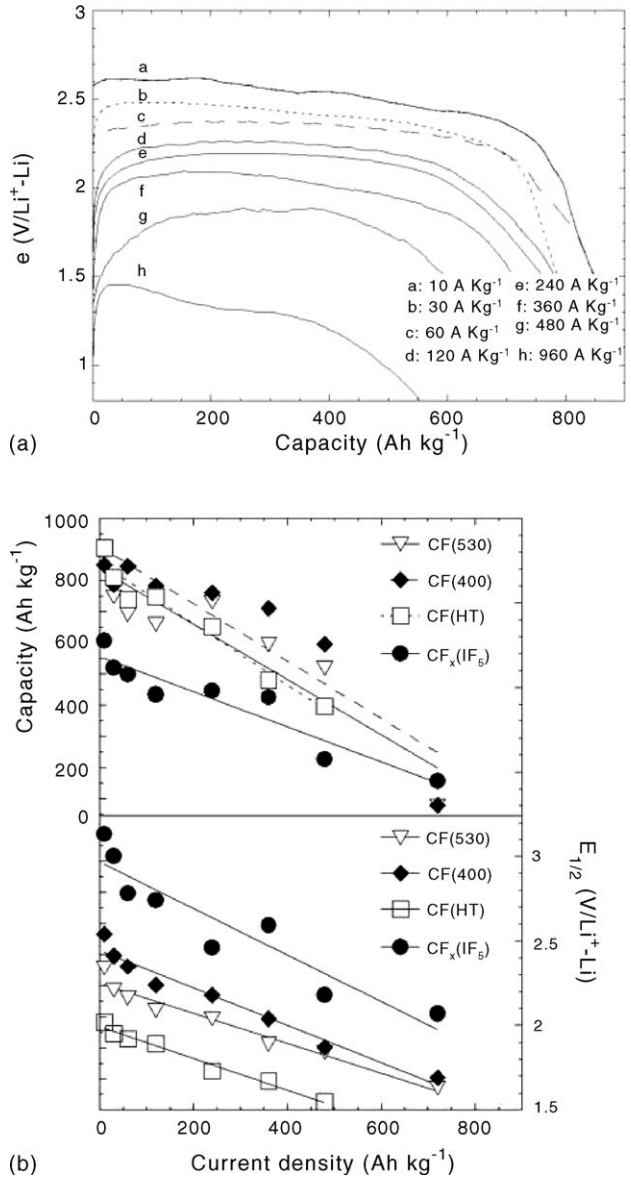

Fig. 4. (a) Galvanostatic discharge curves at room temperature for current density ranged from 10 to 960 A kg^{-1} for CF(400) with 1 M $LiClO_4$/PC as electrolyte. (b) Discharge capacity and average discharge potential as a function of current density for $CF_x(IF_5)$, CF(400), CF(530) and CF(HT). The electrolyte is 1 M $LiClO_4$/PC.

way. A part seems to remain on the electrode surface and/or into the bulk.

3.2.3. Power tests

The electrode performances as a function of the current density, even for high value, is an other key point for application in primary lithium batteries; the investigation of this parameter was also performed. For each graphite fluoride, the increase in the current density results in a decrease of both the discharge voltage and the capacity. Fig. 4a illustrates the effect of the current density on the discharge profile for CF(400). Average discharge potential evolves from 2.54 to 1.88 V for a current density change from 10 to 480 A kg^{-1}, respectively (Table 3).

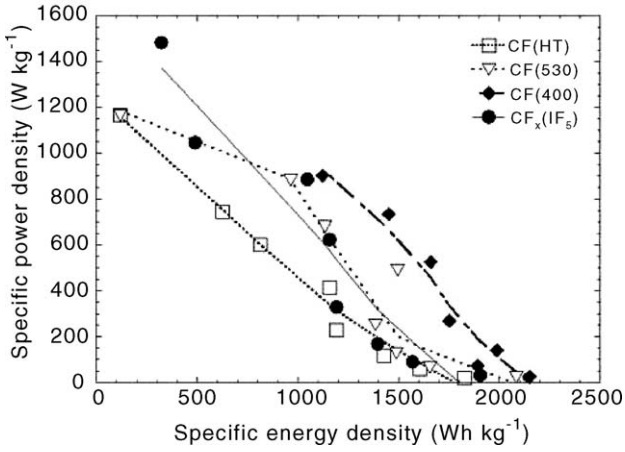

Fig. 5. Ragone plot comparing the performances of all the samples used in primary lithium batteries. The electrolyte is 1 M $LiClO_4$/PC.

The voltage profile for 960 A kg^{-1} is also shown for information although the potential is always lower than the cut-off potential of 1.5 V (applied for the other samples). The observed $E_{1/2}$ is explained by an electrode polarization increasing with current density. The same behavior (not shown here) is observed for the other compounds. The gap of the average potential discharge measured for the two current densities of 10 and 480 A kg^{-1} is 0.47, 0.50, 0.66 and 0.95 for CF(HT), CF(530), CF(400) and $CF_x(IF_5)$, respectively. This fact is related to the difference of the conductivity for these different materials. As shown in Fig. 4b, discharge potential evolution with current density are almost linear. Not surprisingly, whatever the current density, the average discharge potentials keep the same order, from lower to higher values for the following order of the sample: CF(HT), CF(530), CF(400) and $CF_x(IF_5)$. The situation is less evident for capacity dependence, except for $CF_x(IF_5)$ for which capacity is always lower than for the other, the capacities values are interlaced and differ from an hypothetic linear fit. Moreover, capacities for CF(400) and CF(530) are about the same than commercial CF(HT), this, associated with a higher discharge potential, suggests important potentiality for future commercial uses.

A Ragone plot, representation of specific power density E_s (W kg^{-1}) versus specific energy density P_s (Wh kg^{-1}) (Fig. 5), allows a comparison of the performances of each material under different current densities. From discharge curves, the experimental values of E_s ($E_s = C \times E_{1/2}$) and P_s ($P_s = d \times E_{1/2}$) are easily obtained; C and d are the discharge capacity (Ah kg^{-1}) and the current density (A kg^{-1}), respectively. For a better comprehension, Table 3 collects all the discharges characteristic for each current density. In comparison with conventional CF(HT), our new graphite fluorides (treated or untreated) exhibit higher energy densities. Moreover, refluorination leads to an improvement of energy density (≈2100 Wh kg^{-1}). The most important power density (>1500 W kg^{-1}) is obtained for non-refluorinated $CF_x(IF_5)$ whereas the most interesting couple energy–power is reached for CF(400); this point can be explained by both a higher capacity and a higher average potential whatever the current density.

Table 3
Galvanostatic characteristics of Li/CF(HT), Li/CF(530), Li/CF(400) and Li/$CF_x(IF_5)$ batteries obtained at room temperature

Sample	Current density ($A\,kg^{-1}$)	$E_{1/2}$ (V)	Capacity ($Ah\,kg^{-1}$) (at 1.5 V)	Specific energy ($Wh\,kg^{-1}$)	Specific power ($W\,kg^{-1}$)
CF(HT)	10	2.02	905	1828	20
	30	1.96	820	1607	59
	60	1.93	740	1428	116
	120	1.89	630	1191	227
	240	1.73	670	1159	415
	360	1.67	587	980	601
	480	1.55	403	635	744
CF(530)	10	2.34	891	2085	23
	30	2.21	749	1655	66
	60	2.16	689	1488	130
	120	2.10	660	1386	252
	240	2.04	733	1495	490
	360	1.89	600	1134	680
	480	1.84	524	964	883
	720	1.62	73	118	1166
CF(400)	10	2.54	848	2149	25
	30	2.41	785	1892	72
	60	2.35	846	1988	141
	120	2.24	782	1752	269
	240	2.19	758	1660	526
	360	2.04	711	1450	734
	480	1.88	597	1122	902
$CF_x(IF_5)$	10	3.13	609	1906	31
	30	3.01	522	1571	90
	60	2.80	499	1397	168
	120	2.74	435	1192	329
	240	2.59	447	1158	622
	360	2.46	426	1048	886
	480	2.18	225	490	1046
	720	2.06	157	323	1483

Li//1 M $LiClO_4$/PC//CF_x.

4. Conclusion

Semi-covalent and covalent fluorinated graphites obtained from different ways have been synthesized and their bondings have been studied. When the temperature of synthesis (or of refluorination) increases, the NMR and IR data show clearly an increase of the covalence character of the C–F bond.

Electrochemical performances have been then studied, the relationship between average discharge potential and covalence of the C–F bond has been underlined, the higher the covalence, the smaller the average potential. The average potential is 2.02 and 3.13 V for CF_x with covalent and semi-covalent C–F bondings, respectively. Moreover, this potential is higher for upper discharge temperature, for example, in the case of CF(HT), when the temperature is increased from room temperature to 60 °C the potential changes from 2.02 to 2.30 V. Ageing tests reveal that a good ionic conductive salt ($LiClO_4$) associated to a mixed solvent such as EC–PC improves the electrochemical properties. In terms of energy and power density delivered, a good agreement is obtained for CF(400) due to simultaneous large discharge capacity and average potential, for a current density of $360\,A\,kg^{-1}$, the discharge capacity and the average potential are $711\,Ah\,kg^{-1}$ and 2.04 V, respectively. So, this kind of graphite fluoride seems to be promising for a future marketing.

Acknowledgements

This present work was partly supported by a CNRS/FNRS-DGRI Collaborative Research Grant (Centre National de la Recherche Scientifique (FRANCE)/Commissariat Général des Relations Internationales—Fonds National de la Recherche Scientifique (BELGIUM), number 18 205 DUBOIS-MASIN).

References

[1] R. Yazami, in: T. Nakajima (Ed.), Fluorine–Carbon and Fluoride–Carbon Materials: Chemistry, Physics, and Applications, Marcel Dekker, New York, 1995, pp. 251–281.
[2] N. Watanabe, Solid State Ionics 1 (1980) 87–110.
[3] T. Nakajima, N. Watanabe, in: T. Nakajima (Ed.), Graphite Fluorides and Carbon–Fluorine Compounds, CRC Press, Boca Raton, FL, 1991, pp. 84–89.
[4] R. Yazami, A. Hamwi, Solid State Ionics 28–30 (1988) 1756–1761.
[5] R. Hagiwara, W. Lerner, N. Bartlett, T. Nakajima, J. Electrochem. Soc. 135 (1988) 2393–2394.
[6] T. Nakajima, M. Koh, V. Gupta, B. Zemva, K. Lutar, Electrochim. Acta 45 (2000) 1655–1661.
[7] W. Rüdorff, G. Rüdorff, Chem. Ber. 80 (1947) 417–423.
[8] T. Nakajima, in: T. Nakajima (Ed.), Fluorine–Carbon and Fluoride–Carbon Materials: Chemistry, Physics, and Applications, Marcel Dekker, New York, 1995, pp. 11–31.

[9] A.M. Panich, T. Nakajima, S.D. Goren, Chem. Phys. Lett. 271 (1997) 381–384.
[10] A. Hamwi, M. Daoud, J.C. Cousseins, Synth. Met. 26 (1988) 89–98.
[11] A. Hamwi, R. Yazami, Patent WO90/07798.
[12] O. Ruff, O. Bretschneider, F.Z. Ebert, Anorg. Allg. Chem. 217 (1934) 1–19.
[13] Y. Kita, N. Watanabe, Y. Fuji, J. Am. Chem. Soc. 101 (1979) 3832–3841.
[14] K. Guérin, J.P. Pinheiro, M. Dubois, Z. Fawal, F. Masin, R. Yazami, A. Hamwi, Chem. Mater. 16 (2004) 1786–1792.
[15] M. Dubois, K. Guérin, J.P. Pinheiro, Z. Fawal, F. Masin, A. Hamwi, Carbon 42 (2004) 1931–1940.
[16] A. Hamwi, M. Daoud, J.C. Cousseins, Synth. Met. 30 (1989) 23–31.
[17] P. Hany, R. Yazami, A. Hamwi, J. Power Sources 68 (1997) 708–710.
[18] M.J. Root, R. Dumas, R. Yazami, A. Hamwi, J. Electrochem. Soc. 148 (2001) 339–345.
[19] K. Guérin, R. Yazami, A. Hamwi, Electrochem. Solid State Lett. 7 (2004) 159–162.
[20] T.R. Krawietz, J.F. Haw, Chem. Commun. 19 (1998) 2151–2152.
[21] A.M. Panich, T. Nakajima, Mol. Cryst. Liq. Cryst. 340 (2000) 77–82.
[22] J. Giraudet, M. Dubois, K. Guérin, J.P. Pinheiro, A. Hamwi, W.E.E. Stone, P. Pirotte, F. Masin, J. Solid State Chem. 178 (2005) 1262–1268.
[23] A. Hamwi, M. Daoud, D. Djurado, J.C. Cousseins, Z. Fawal, J. Dupuis, Synth. Met. 44 (1991) 75–83.
[24] H. Selig, W.A. Sunder, M.J. Vasile, F.A. Stevie, P.K. Gallagher, L.B. Ebert, J. Fluorine Chem. 12 (1978) 397–412.
[25] R.K. Heenan, R. Robiette, J. Mol. Struct. 55 (1979) 191–197.
[26] K.O. Christe, W.W. Wilson, Inorg. Chem. 28 (1989) 3275–3277.